



24th ABCM International Congress of Mechanical Engineering December 3-8, 2017, Curitiba, PR, Brazil

# COBEM-2017-1066

# Trailing edge formation during slot coating of rectangular patches

#### D. Maza

#### M. S. Carvalho

Department of Mechanical Engineering Pontifical Catholic University of Rio de Janeiro - PUC-Rio danmerm@puc-rio.br, msc@puc-rio.br

Abstract. Coating of discrete patches onto a moving substrate is becoming more common as a variety of new products are developed, ranging from adhesives, pharmaceutical patches, batteries and fuel cell membranes. Coating individual discrete shapes can reduce waste that comes from converting processes and can provide desired functionality, such as in the case of anode and cathode thin-film lithium batteries, at which the uncoated boundary is needed to prevent short circuit. For coating rectangular patches, intermittent slot die coating is the preferred method. Machine-direction dry lanes can be obtained by blocking the feed slot with internal inserts, diverting the liquid flow away from these lanes. Cross-web dry lanes can be obtained by starting and stopping the flow out of the coating die. Controlling the flow start-up and shutdown to produce sharp and uniform leading and trailing edges is very challenging. In this work, we analyze the trailing edge formation during slot coating process of rectangular patches and how the operating conditions, die geometry and liquid properties affect the trailing edge of the coated patch. The results show that the uniformity of the coating boundary can be improved by changing the die shoulder angle and wetting characteristics.

Keywords: Patch coating, coating flow, computational fluid dynamics, fluid dynamics

## 1. INTRODUCTION

Coating of discrete patches onto a moving substrate is becoming more common as a variety of new products are developed, ranging from adhesives, pharmaceutical patches, batteries and fuel cell membranes. Coating individual discrete shapes can reduce waste that comes from converting processes and can provide desired functionality, such as in the case of anode and cathode of thin-film lithium batteries, as mentioned by (Schmitt *et al.*, 2014), at which the uncoated boundary is needed to prevent short circuit. Patch coating or intermittent coating is a method used to deposit rectangular patterns on a continuously passing web by different coating methods as cited by (Kim *et al.*, 2009). Specifically in the case of slot die patch coating, the shape is usually a rectangle as sketched in Fig.1.

Coating patches of uniform thickness is extremely challenging. The leading edge of the patch is formed as the substrate is wetted and coating bead is formed. The trailing edge is formed as the liquid dewets the substrate and the coating bead is removed without leaving residue. In summary, path coating can be viewed as successive start-ups and shut-downs with a fast steady state flow in between them. These processes have to be as fast as possible to avoid thickness variation on the deposited patch. Moreover, Three dimensional instabilities may grow leading to a wavy contact line along the cross-web direction.

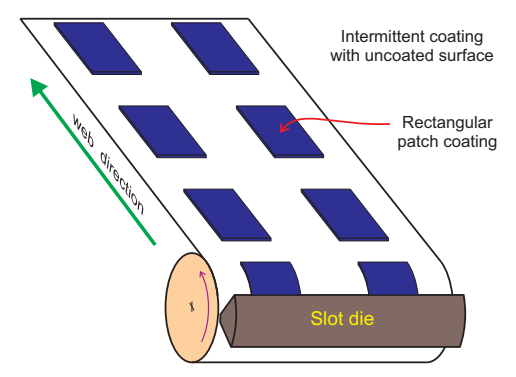


Figure 1. Sketch of slot die patch coating where the shape is usually a rectangle

The fast start-up and shut-down of the flow can be achieved in different ways. (Milbourn and Barth, 1994) proposed the use of a pneumatic single three way valve as shown in Fig.2. The same concept was extended to different valve setups

((Watanabe *et al.*, 1998) and (Iwashita *et al.*, 1999)). The use of a variable die cavity was proposed by (Schmitkons *et al.*, 1998) and (Sakai *et al.*, 2002), (Szczepaniak *et al.*, 2014) and (Vries, 2014) used the fast change on the die position to promote a rapid growth and break-up of the coating.

Despite the industry use, the different methods have not been extensively analyzed from the fundamental point of view.

An experimental analysis on operating windows of sot die patch coating was presented by (Yang *et al.*, 2004). The main conclusion was that the defects characteristics observed at the leading and trailing edge were related to two critical phenomena steady state: Coatability windows and the process response time of the die.

The film thickness profile along the downweb direction is directly related to the transient pressure response in the liquid feeding system as showed by (Kim *et al.*, 2009). As the by-pass valve was opened and closed. The pressure in the in the feeding system did not reached the constant value or zero immediately. The observed transient response could be associated with the liquid viscoelastic behavior, liquid compressibility due to entrapped micro air bubbles, inertial or capillary effects.

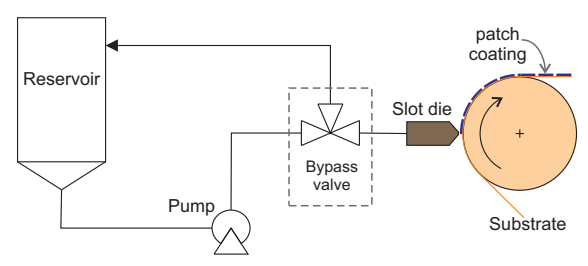


Figure 2. Pneumatic valves with a single three-way valve used in slot die patch coating

An experimental analysis and an analytical model to describe intermittend slot die coating was presented recently by (Schmitt *et al.*, 2015). The results show that the transient during the flow shut-down step is longer, which leads to a long trailing edge as sketched in Fig. 3. This is usually minimized by either reverting the pumping flow out of the feed slot. i.e sucking back the liquid in the coating into the feed slot, or by rapidly opening the coating gap, promoting a fast break-up of the coating bead.

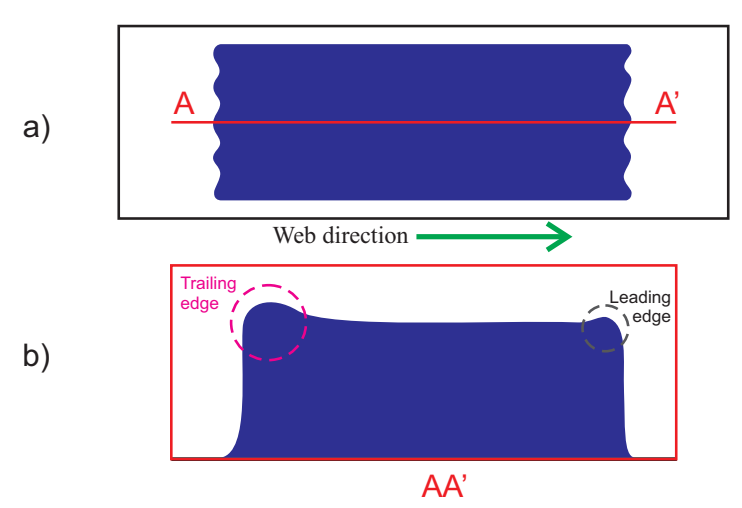


Figure 3. Rectangular Patch coating: a)Top view b)Side view and its characteristics defects on patch coating: heavy leading and trailing edge defects

Despite its use by the industry, fundamental understanding of the flow during the shut-down step of intermittent coating us still limited.

The transient response during the flow shut-down phase and consequently the length of the trailing edge is a function of the dynamics of the free surfaces that bounds the coating bead.

Fundamental understanding of the transient flow after the flow rate is set to zero until the coating bead breaks can lead to optimization of the process and reduction of the trailing edge in patch coating. This is the main goal of this analysis. The transient free surface problem is solved by the Galerking-Finite Element method. The effect of liquid properties, die lip geometry and wetting characteristics on the bead break-up process and consequently on the trailing edge length are determined in order to determine process conditions that would lead to patches of coating with sharped trailing edge.

#### 2. MATHEMATICAL MODEL

The transient flow in the coating bead during shutdown process was described by the transient, two-dimensional, incompressible free surface flow of a Newtonian liquid.

The flow domain at which the governing equations are solved is sketched in Fig.4a. It is bounded by the upstream and downstream free surfaces, the die lips and moving substrate. The distance between the coating die and the moving substrate is called the coating gap H. In the analysis presented here,  $H=127\mu\mathrm{m}$ . The length of the downstream die lip and the feed slot height are equal to 1.0 mm and 0.5 mm respectively. In the edge of the downstream corner die has a radius of curvature of  $R=10\mu\mathrm{m}$  avoiding singularities and so the contact angle measured at the surface remain constant. To simplify the upstream static contact line motion during the transient flow, we did not include the feed slot in the flow domain. More details of the geometry is shown in Fig. 4a.

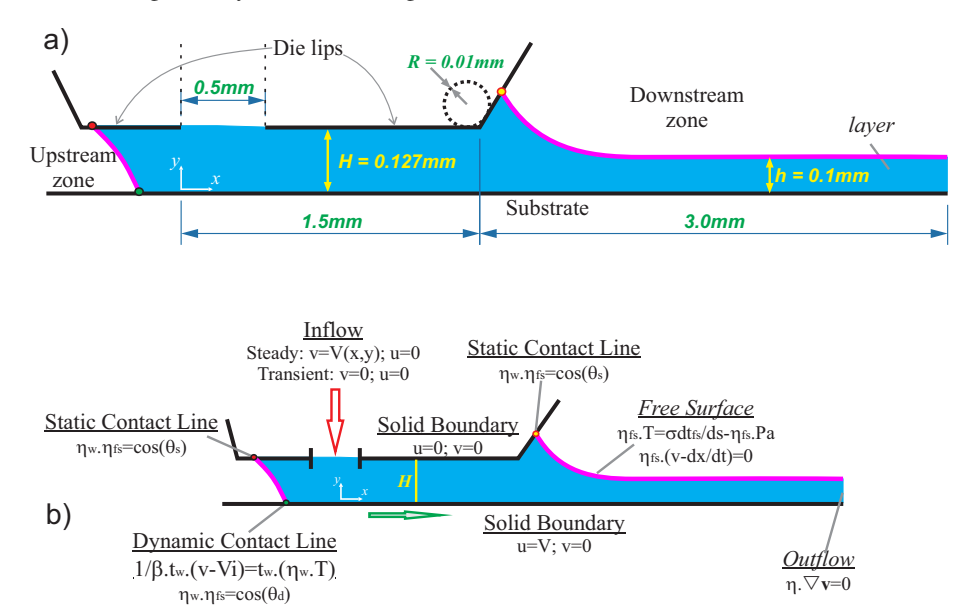


Figure 4. a) Sketch of flow domain into the coating bed where the characteristic dimensions are in mm and b)Boundary condition for theoretical modeling

# 2.1 Governing Equations and Boundary Conditions

The velocity  $\mathbf{v}$  and pressure p fields of the transient, two-dimensional, incompressible flow of a Newtonian liquid are governed by the continuity and momentum conservation equations:

$$\nabla \cdot \mathbf{v} = 0; \tag{1}$$

$$\rho \left( \frac{\partial \mathbf{v}}{\partial t} + \mathbf{v} \cdot \nabla \mathbf{v} \right) - \nabla \cdot \mathbf{T} = 0.$$
 (2)

Where  $\rho$  is the liquid density. The total stress tensor for Newtonian liquids is  $\mathbf{T} = -p + \mu [\nabla \mathbf{v} + (\nabla \mathbf{v})^T]$  where  $\mu$  is the liquid viscosity.

Boundary conditions are needed to solve the Navier-Stokes system, they are shown in Fig.4b.

At the synthetic outflow plane, placed 40H downstream of the injection feed as shown in Fig.4b, the flow is considered fully-developed:

$$\mathbf{n} \cdot \nabla \mathbf{v} = 0. \tag{3}$$

The no-slip and no-penetration conditions applies along the die walls and the moving substrate.

$$u = V$$
,  $v = 0$ , along the substrate, (4)

$$u = 0$$
,  $v = 0$ , along the die walls. (5)

At the dynamic contact point, where the upstream meniscus meets the moving web, Navier-slip condition is used instead of no-slip condition and a dynamic contact angle  $\theta_{dyn}$  is imposed:

$$\frac{1}{\beta} \mathbf{t}_w \cdot (\mathbf{v} - V_0 \mathbf{i}) = \mathbf{t}_w \cdot (\mathbf{n}_w \cdot \mathbf{T}), \qquad \mathbf{n}_w \cdot \mathbf{n}_{fs} = \cos(\theta_{dyn}). \tag{6}$$

The upstream and downstream static contact lines are free to move along the upstream die lip and downstream die shoulder with a prescribed static contact angles  $\theta_s$ :

$$\mathbf{n}_w \cdot \mathbf{n}_{fs} = \cos(\theta_s). \tag{7}$$

It is important to note that the previous equation imposes a constant contact angle, regardless of the wetting velocity and neglects contact angle hysteresis. This approach is only strictly valid for low wetting velocities, but was used here for simplicity. We assume that despite utilizing such a simplistic slip model, the essential features of trailing edge formation is captured.

Along the upstream and downstream gas-liquid interfaces, the traction in the liquid balances the capillary pressure and there is no mass flow rate across the interface. It is assumed that the gas viscosity is much smaller than the liquid viscosity, leading to vanishing shear stress along the gas-liquid interface:

$$\mathbf{n}_{fs} \cdot \mathbf{T} = \sigma \frac{d\mathbf{t}_{fs}}{ds} - \mathbf{n}_{fs} \, p_0, \tag{8}$$

$$\mathbf{n}_{fs} \cdot \left( \mathbf{v} - \overset{\circ}{\mathbf{x}} \right) = 0, \tag{9}$$

where  $\sigma$  is the liquid surface tension,  $\mathbf{t}_{fs}$  and  $\mathbf{n}_{fs}$  are the local unit tangent and unit normal vectors to the free surface,  $d\mathbf{t}_{fs}/ds$  represents the curvature of the meniscus,  $p_0$  is the pressure of the gas, and  $\mathbf{x}$  is the mesh velocity. At the upstream and downstream free surface, the gas pressure was set atmospheric, that is  $p_0 = P_{atm}$ .

In order to describe the coating bead break-up dynamics avoiding the complex change of topology of the upstream free surface as the static contact line jumps from the upstream to the downstream die lip, we assume that after the flow shut-down the flow rate is q=0 for t>0 and the feed slot exit behaves as a wall with u=v=0.

An initial condition is needed in order to solve the transient flow. In this work, the steady state solution of the flow was used as the initial condition for the transient analysis. At the inlet plane, we assumed a parabolic velocity profile with a prescribed flow rate q.

$$v = -\frac{6q(t)}{H^3} \left[ Hy - y^2 \right], \text{ for } t = 0$$
 (10)

Slot die patch coating can be used for different applications, from very viscous non Newtonian dispersions to low viscosity Newtonian liquids; from very thin films to relatively thick layers. The operating parameters of slot die patch coating process, their respective range covering different applications and the values considered as base case in this analysis are presented in Table 1. The static contact angles between the downstream and upstream free surfaces with the die shoulders were considered equal. The process variables can be grouped in the dimensionless parameters listed in Table 2. The values of the dimensionless number for the base case are also shown. They are close to the values considered in the analysis presented by Schmitt *et al.* (2015) for lithium-ion battery electrodes.

Table 1. Parameters for a typical two layer slot coating

Parameter	Unit	Symbol	Range	Base Case
Gap width	$\mu m$	Н	50 - 200	127
Web speed	$ms^{-1}$	V	0 - 1.5	0.01
Pressure difference	kPa	$P_{vac}$	0 - 10	0
Dynamic contact angle	0	$ heta_d$	140 - 160	120
Static contact angle	0	$\theta_{s-u} = \theta_{s-d}$	5 - 180	95
Density	$kgm^{-3}$	ho	900 - 1300	$\rho = 1000$
Viscosity	mPa.s	$\mu$	0.5 - 1000	$\mu = 470$
Surface tension	mN/m	$\sigma$	20 - 60	$\sigma = 53$
Film thickness	$\mu m$	h	20 - 150	h = 100

Table 2. Dimensionless parameters

Group	Definition	Base Case	
Capillary number	$Ca = \mu V/\sigma$	0.09	
Reynolds number	$Re = \rho V H / \mu$	$1.9 \times 10^{-3}$	
Vacuum Pressure	$Vac = P_{vac}H/\sigma$	0	
Film thickness ratio	G = H/h	1.27	

#### 3. SOLUTION METHOD

Predicting the trailing edge formation during patch coating involves determining the evolution of the upstream and downstream free surfaces along the die surface. The flow domain is unknown a priori and changes with the time. To solve a free-boundary problem by means of standard techniques for boundary value problems, the set of differential equations and boundary conditions posed in the unknown physical domain have to be transformed to an equivalent set defined in a known, fixed computational domain. Details of this method are discussed elsewhere by Christodoulou and Scriven (1992), de Santos (1991), Romero and Carvalho (2008) and Maza and Carvalho (2014).

The mapping used here is the one described previously by de Santos (1991). The inverse mapping is governed by a system of elliptic differential equations identical to those encountered in the dilute regime of diffusional transport.

$$\nabla \cdot D_{\xi}(\xi, \eta) \nabla \xi = 0, \ \nabla \cdot D_{\eta}(\xi, \eta) \nabla \eta = 0. \tag{11}$$

 $D_{\xi}$  and  $D_{\eta}$  are mesh diffusivities which control the steepness of gradients in the node-spacing by adjusting the potentials  $\xi$  and  $\eta$ . Curves of constant  $\xi$  and  $\eta$  define the boundaries of elements used to describe the domain. The cross point of these curves sets the position of a node. Boundary conditions are needed to solve the second-order differential equations (11). Solid walls and inflow and outflow planes are described by the function that defines their geometry and nodes were distributed along them by a specified stretching function. The location of the free surfaces and interlayer are implicitly determined by the corresponding kinematic conditions Eq. (9). The discrete version of the mapping equations is generally referred to as mesh generation equations. Detailed procedure and boundary conditions for mesh equation are discussed in de Santos (1991)

In transient problems, the frame of reference lies across the space-time domain for which the physical grid points are constantly updated in time. Therefore, time derivative at fixed Eulerian locations in space needs to be transformed to time derivative at fixed iso-parametric coordinates. The time derivative of the nodal position, i.e. the mesh velocity, needs to be considered in the momentum equation Christodoulou and Scriven (1992):

$$\rho \left[ \mathring{\mathbf{v}} + (\mathbf{v} - \mathring{\mathbf{x}}) \cdot \nabla \mathbf{v} \right] - \nabla \cdot \mathbf{T} = 0, \tag{12}$$

The system of governing equations together with the appropriate boundary conditions and initial condition was solved by Galerkin's method with quadrilateral finite elements. Details on the finite element discretization were discussed in Maza and Carvalho (2014).

Once all the variables are represented in terms of the basis functions, the system of partial differential equations reduces to a set of ordinary differential and algebraic equations that describe the evolution of the coefficients with time:

$$\mathbf{R}(\mathbf{u}, \dot{\mathbf{u}}, \mathbf{f}(t)) = 0,\tag{13}$$

where  $\mathbf{R}$  is the set of weighted residual equations,  $\mathbf{u}$  is the vector of basis functions' coefficients,  $\dot{\mathbf{u}}$  is their time derivatives, and  $\mathbf{f}$  a vector that contain all the input parameters (physical properties, geometry of the flow and boundary condition information).

As mentioned before, the initial condition of the transient flows related to the shutdown process was the steady-state flow with a uniform film thickness. Therefore, the first step of the analysis was the solution of the steady state flow. The system of ordinary differential-algebraic equations is reduced to simultaneous algebraic non-linear equations for the coefficients of the basis functions of all the fields

$$\mathbf{R}(\mathbf{u}, \mathbf{f_0}) = 0,\tag{14}$$

which was solved by Newton's method, that requires the evaluation of the Jacobian matrix. The vector  $\mathbf{f_0}$  contains the input parameters of the steady-state flow.

The temporal discretization of the set of ordinary differential-algebraic equations follows the first-order fully implicit Euler method. Fig. 5a shows the film thickness evolution measured at the synthetic outflow plane for three different meshes (M1 = 2940, M2 = 3729 and M3 = 4563 elements). Fig. 5b shows the trailing edge formation at the break-up time where is possible to see the thick coating region and the amount of liquid at the end of the coated patch. A mesh M1 with 57,000 degrees of freedom was considered satisfactory and was used to obtain the solutions reported here. A time step of  $\Delta t \approx 2 \times 10^{-5}$  was adopted in all computations.

## 4. RESULTS

Effect of process condition in the bead break-up and film thickness variation is analyzed here by comparing transient flow predictions using three different die geometries, shown in Fig.6. Each configuration has a different die shoulder angle  $\phi$ :  $65^{o}$ ,  $45^{o}$ , and  $80^{o}$ . Transient solution is computed until the both contact lines in the die lip merge into a single point from which the liquid detaches from the die surface.

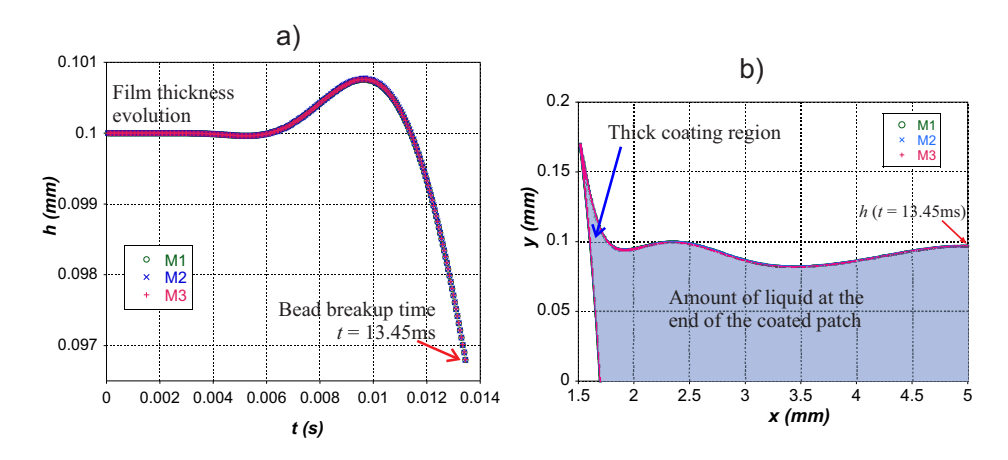


Figure 5. Mesh test analysis related on a) film thickness evolution until the bead break-up condition is achieve and b) profile of the amount of liquid at the end of the coated patch

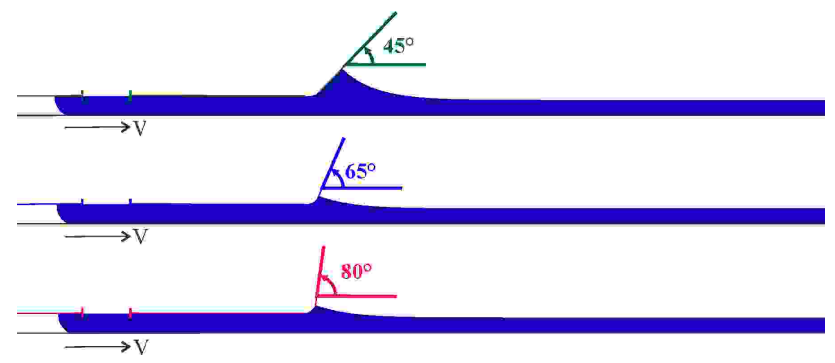


Figure 6. Die geometries with three different die shoulder angle:  $\phi = 45^{\circ}$ ,  $\phi = 65^{\circ}$  and  $\phi = 80^{\circ}$ .

The effect of the die lip geometry was analyzed with the following conditions: static contact angles equal to  $\theta_{s-u}=$ 

 $\theta_{s-d}=95^o$ , dynamic contact angle at the substrate is set at  $\theta_{d-u}=60^o$ ,  $Ca=9\times 10^{-2}$  and  $Re=1.9\times 10^{-3}$ . Figure 7 shows the evolution of the film thickness profile h'=h/h(t=0) as a function of dimensionless time t' = tV/h(t=0). The flow rate was set to zero at t'=0.

The film thickness at the outflow plane remains constant up to t'=10. It then grows, reaching a maximum value at around t'=23 before falling until the bead break-up, as shown in Fig.7.

The breakup time is shorter for the die with the larger shoulder angle, i.e.  $\phi = 80$ . The break-up time varied from t' = 36 for  $\phi = 45^{\circ}$  to  $t' = 31.2 \ \phi = 80^{\circ}$ .

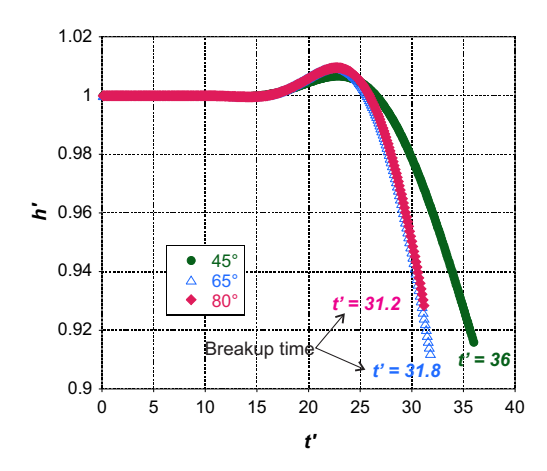


Figure 7. Evolution of dimensionless film thickness profile h' along the time t' for different die shoulder angle

Figure 8a shows the evolution of both free surface for  $\phi=45^{\circ}$ . The steady state configuration is at t'=0. After the flow is shut-down, both free surfaces move towards the downstream die lip corner (t'=21). At the certain time, the downstream contact line changes direction and starts to move along the die shoulder (t'=27). The upstream contact line continues to move downward along the die surface until it merges with the downstream contact line at t'=36. This is the configuration at break-up. Figure 8b shows the upstream and downstream static contact line position as a function of time t' along the die lip surface until the break-up conditions is achieve where both line merge into a single point.

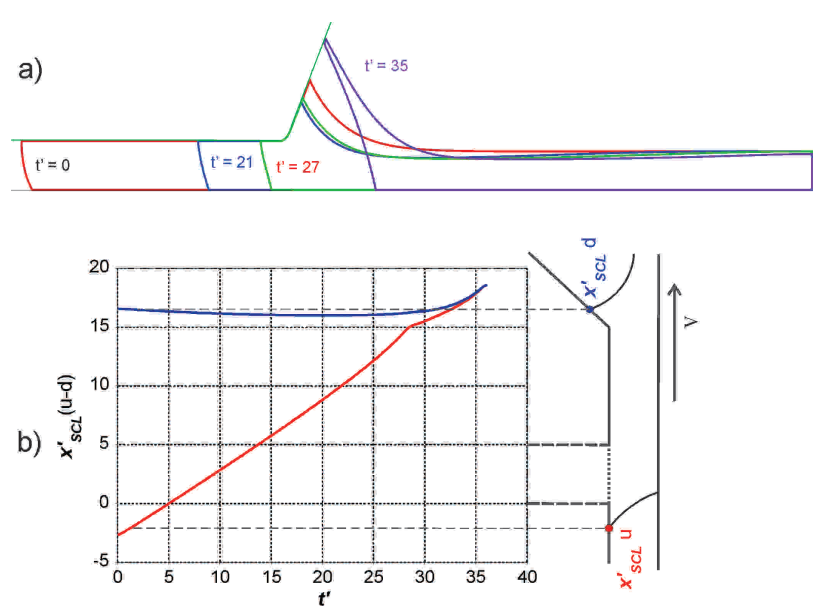


Figure 8. a) Sequence of profile of the amount of liquid at the end of the coated patch along time toward to break up condition at  $Re=1.9\times 10^{-3}$ ,  $Ca=9\times 10^{-2}$  and  $\phi=45^{o}$  b) Evolution of the upstream and downstream static contact line position until they merge into a single point

The liquid configuration at break-up for the three die geometries considered is shown in Fig.9. The amount of liquid at the end of the coated patch for the  $\phi=45^o$  die is larger than the other two configurations. For  $\phi=45^o$ , not only the trailing edge is longer, but also a small region of the thick coating is formed.

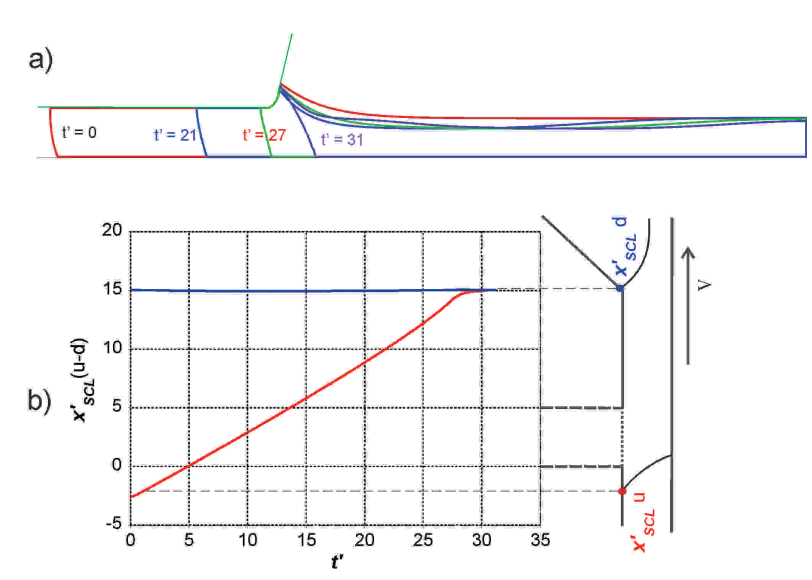


Figure 9. a) Sequence of profile of the amount of liquid at the end of the coated patch along time toward to break up condition at  $Re=1.9\times 10^{-3}$ ,  $Ca=9\times 10^{-2}$  and  $\phi=80^{o}$  b) Evolution of the upstream and downstream static contact line position until they merge into a single point

The results show that the length of the trailing edge and the film thickness profile can be optimized by simply changing

the die lip geometry. A sharper die corner ( $\theta = 65^{\circ}$  and  $\theta = 80^{\circ}$ ) promotes pinning of the contact line and hinders its motion along the die surface, leading to a faster break-up.

The results presented before show that the upstream and downstream static contact line motion along the die surface is directly related to the break-up dynamics. Another way to control this motion is by changing the wettability characteristics of the liquid-surface interaction.

Fig. 10a shows the bead break-up configuration for  $\theta_{s-u}=\theta_{s-d}=95^o, 120^o$  and  $160^o$  for  $\phi=45^o$  die lip geometry. The predictions were obtained at  $Ca=9\times 10^{-2}, Re=1.9\times 10^{-3}$  and  $\theta d-u=60^o$ . As the die surface becomes more non-wettable, i.e. as  $\theta_{s-u}$  rises, the contact line motion is hindered and the upstream and downstream contact line meet near the die corner. The volume of liquid at the end of the patch is minimized and the film thickness is more uniform. The length of the trailing edge is also minimized, as shown in the thick coating region in Fig.10a. The behavior is also similar for the other two die lip geometry explored, e.g.  $\phi=65^o$  and  $\phi=80^o$ , as shown in Fig. 10 b and c respectively. The figure shows the bead break-up configuration for all the three geometries and contact angle explored.

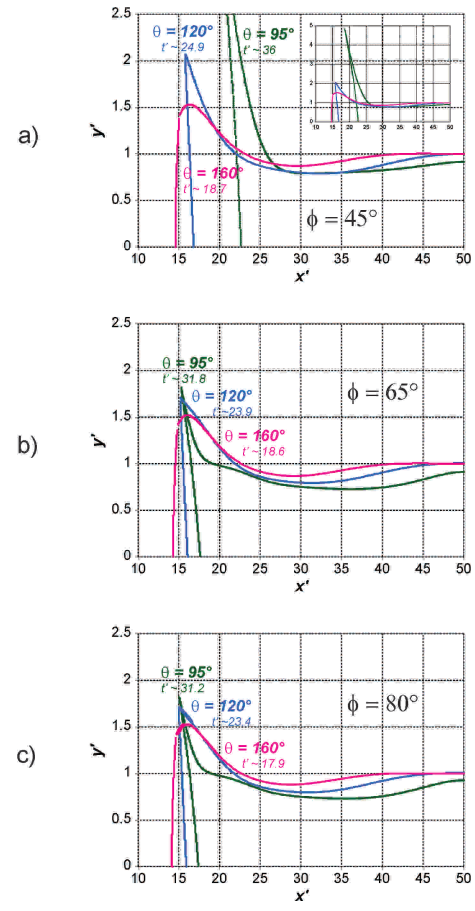


Figure 10. Die wetting effect on the profile of the amount of liquid at the end of the coated patch. a)  $\phi = 45^o$ , b)  $\phi = 65^o$  and c)  $\phi = 80^o$ 

## 5. FINAL REMARKS

The trailing edge formation during the shutdown process of intermittent slot die coating at different operating parameter were analyzed here by solving the momentum and continuity equation system for transient, two-dimensional, free surface flows.

The results show that film thickness profile is directly related to the static contact line motion along the die surface after the flow rate fed to the die vanishes.

The break-up time and consequently the length of the trailing edge can be minimized by hindering the contact line motion. In the cases analyzed here, this was done by either making the downstream die corner sharper, which promotes contact line pinning, or by making the die surface more non-wetting.

#### 6. ACKNOWLEDGEMENTS

This work was funded by CNPq (Brazilian Research Council), FAPERJ and by the Industrial Partnership for Research in Interfacial and Materials Engineering (IPRIME) of the University of Minnesota.

#### 7. REFERENCES

- Christodoulou, K. and Scriven, L., 1992. "Discretization of free surface flows and other moving boundary problems". *Journal of Computational Physics*, Vol. 99, pp. 39 55.
- de Santos, J., 1991. *Two-phase cocurrent downflow through constricted passages*. Ph.D. thesis, University of Minnesota, MN. US.
- Iwashita, Y., Endo, S. and Morimoto, K., 1999. "Intermittent coating method and apparatus therefor". *U. S. Patent*, Vol. 5989622A.
- Kim, S., Kim, J., Ahn, K. and Lee, S., 2009. "Rheological perspectives of industrial coating process". *Korea-Australia Rheology Journal*, Vol. 21, pp. 83–89.
- Maza, D. and Carvalho, M., 2014. "Transient response of two-layer slot coating flows to periodic disturbances". *AIChE Journal*, Vol. 61, pp. 1699 1707.
- Milbourn, T. and Barth, J., 1994. "Method of applying discrete coating patches on a moving web". *U. S. Patent*, Vol. 5360629.
- Romero, O. and Carvalho, M., 2008. "Response of slot coating flows to periodic disturbances". *Chemical Engineering Science*, Vol. 63, pp. 2161 2173.
- Sakai, Y., Yoshikawa, T. and Akinori, I., 2002. "Intermittent coating system and intermittent coating method". *U. S. Patent*, Vol. 6455105B1.
- Schmitkons, J., Turner, J., Zupan, M., Rivas, A., Benecke, J., Cieplik, A., Burmester, T. and Boger, B., 1998. "Snuff back controlled coating dispensing apparatus and methods". *U. S. Patent*, Vol. 5733597A.
- Schmitt, M., Diehm, R., Scharfer, P. and Schabel, W., 2015. "An experimental and analytical study on intermittent slot die coating of viscoelastic battery slurries". *Journal of Coatings Technology and Research*, Vol. 12, pp. 927–938.
- Schmitt, M., Scharfer, P. and Schabel, W., 2014. "Slot die coating of lithium-ion battery electrodes: Investigations on edge effect issues for stripe and pattern coatings". *Journal of Coatings Technology and Research*, Vol. 11, pp. 57–63.
- Szczepaniak, W., Janssen, F. and Blum, J., 2014. "Device for linear adjustment of machine component, has adjustment unit that is acted on adjustment tape for bending motion, so that the machine component is moved relative to the bearing on linear guide portions". *DE Patent App*, Vol. DE102012110305A1.
- Vries, I.d., 2014. "Intermittent slot die coating of low viscous soulutions". In *International Coating Science and Technology Symposium ISCST2014*). San Diego, CA, USA.
- Watanabe, M., Ueyama, Y., Nakamura, T., Ohana, Y. and Hayashi, T., 1998. "Intermittent coating apparatus, intermittent coating method and manufacturing method of battery electrodes, and non aqueous electrolyte cell". *U. S. Patent*, Vol. 5824156.
- Yang, C., Wong, D. and Liu, T., 2004. "An experimental study on discrete patch coating". *Industrial coating research*, Vol. 5, pp. 43–58.

#### 8. RESPONSIBILITY NOTICE

The following text, properly adapted to the number of authors, must be included in the last section of the paper: The author(s) is (are) the only responsible for the printed material included in this paper.